

Microscopy, 2019, 37–44 doi: 10.1093/jmicro/dfy043 Advance Access Publication Date: 8 October 2018



Review

Structured illumination approaches for super-resolution in plant cells

Sidney L. Shaw*, David Thoms, and James Powers

Department of Biology, Light Microscopy Imaging Center, Indiana University, Bloomington, IN 47405. USA

*To whom correspondence should be addressed. E-mail: sishaw@indiana.edu

Received 6 August 2018; Editorial Decision 20 September 2018; Accepted 1 October 2018

Abstract

The advent of super-resolution techniques in biological microscopy has opened new frontiers for exploring the molecular distribution of proteins and small molecules in cells. Improvements in optical design and innovations in the approaches for the collection of fluorescence emission have produced substantial gains in signal from chemical labels and fluorescent proteins. Structuring the illumination to elicit fluorescence from specific or even random patterns allows the extraction of higher order spatial frequencies from specimens labeled with conventional probes. Application of this approach to plant systems for super-resolution imaging has been relatively slow owing in large part to aberrations incurred when imaging through the plant cell wall. In this brief review, we address the use of two prominent methods for generating super-resolution images in living plant specimens and discuss future directions for gaining better access to these techniques.

Key words: plant, SIM, structured illumination

Super-resolution using structured illumination

Fluorescence microscopy is a remarkably powerful method for exploring the distribution of proteins and small molecules within cells. Coupling a fluorophore to a molecule of interest by chemical or genetic methods produces a high-contrast probe for *in situ* and *in vivo* analyses. The basic design of the episcopic fluorescence microscope, using a dichromatic mirror to reflect excitation energy through the objective lens to the specimen, produces a magnified image of the collected light. While the contrast imparted by fluorescence provides an exceptional means for molecular identification, the nominal resolution of the light microscope is

severely limited when examining molecular assemblies on the scale of a protein. A single fluorescent protein, about 4 nm in size, is transformed by even the best objective lens into a Gaussian-shaped blur spanning almost half a micrometer. Hence, fluorescence microscopy generally reports ensembles of proteins or small molecules with relatively poor precision. The idea of super-resolution is to bring the resolving power of the light microscope closer to the scale of the molecular assemblies of interest within cells.

In wide-field fluorescence microscopy, the specimen is illuminated uniformly to affect a flat field. Uniform illumination excites all of the fluorophores in the field yielding a representative distribution of molecules across the specimen. When we consider each fluorophore pointwise, the resolution of the aberration-free imaging system can be related to the numerical aperture of the lens or solid angle of light collection from each point through a medium. In geometric optics, the rays from a point source are mapped back to a singular position in the image plane by the lens. But the application of wave theory shows us that the light from a far-field point undergoes diffraction. The converging wavefronts undergo interference at the image plane leading to a circular pattern, rather than a singular point, referred to as an Airy disk or point spread function (PSF). The size of the PSF depends upon the wavelength of light, the refractive index of the medium and the aperture size of the lens. The diffraction pattern is described mathematically in the far field by a first-order Bessel function applied to the wavelength and aggregate numerical aperture. This treatment of the point source underpins the commonly

used Rayleigh criterion for optical resolution, where the peak intensity of one Airy disk, centered on the first valley of an adjacent Airy disk, results in just enough contrast to distinguish each as a single peak with adequate signal.

Extending this description to the frequency domain, the numerical aperture of the objective lens acts as a low-pass filter, limiting the spatial frequencies passing through the system related to the higher angle rays from geometric optics (Fig. 1a–d). Recall that the reconstruction of a square wave from a summation of sine waves begins with stronger, low-frequency components and adds progressively higher spatial frequency waves to eventually sharpen the 'square' corners. Analogously, the two-dimensional image or Airy pattern requires higher spatial frequency components passing through the lens aperture, those captured at wider angles from the specimen, to narrow the PSF and increase the resolving power of the system. The principal idea for increasing resolution in the fluorescence microscope through

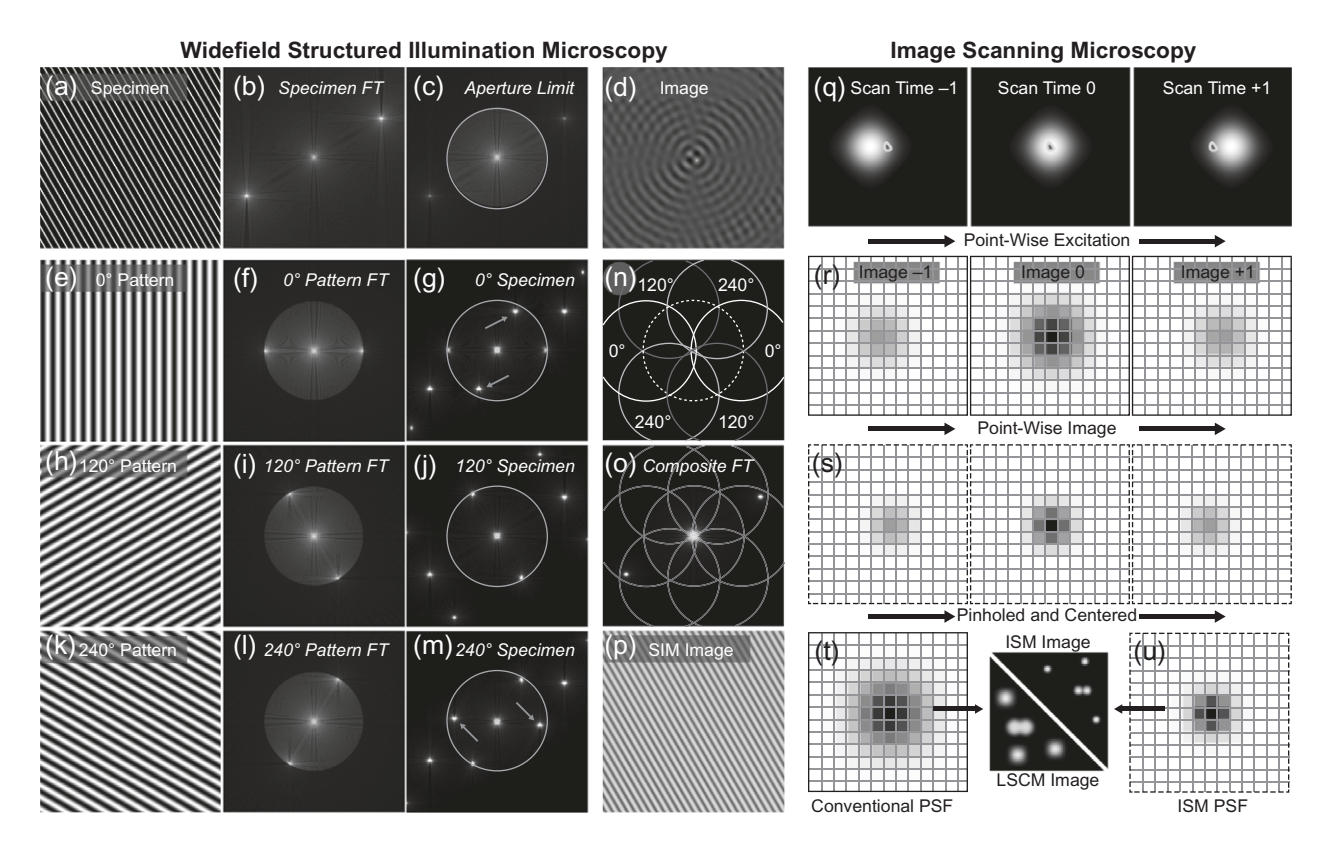


Fig. 1. Overview of wide-field SIM and image scanning microscopy (ISM) for super-resolution. Spatial patterns in the specimen below the resolving power of the objective lens (a) viewed as 2D frequency domain (italic) patterns (b) are low-pass filtered by the objective lens (c—circle), leading to a loss of spatial detail (d). Sinusoidal illumination patterns (e—m), laterally shifted over 3 or 5 positions and rotated to 0°, 120°, 240°, bring new information into the lens aperture. Each real space sine pattern (e, h, k) produces three frequency domain peaks in different orientations (f, i, l) where specimen frequencies are replicated on each of the illumination peaks (g, j, m) bringing new information (arrows in g and m) into the aperture (circle in g, j,m). The new information is extracted from each laterally shifted image based on the phase and the Fourier transformed plus and minus orders are moved in frequency space to positions related to the plus and minus orders of the illumination pattern (n). The composite frequency space image (o) is then backtransformed to recover the real space image (p) with up twice the non-SIM resolution. In an ISM, a scanned excitation beam (q) produces an emission peak with a spatial position and intensity that vary with beam position (r—reversed for clarity). When captured by an array detector (r), each image can be transformed (s) by spatial filtering (i.e. pinholing) and translation with relation to the absolute spatial position of the excitation beam. Compared to the conventional or confocal PSF collected by an integrating point detector (t), the combined ISM image forms a PSF with up to 1.4 fold improved resolution and better photon efficiency (u).

structured illumination is to bring more high-frequency information into the lens aperture (Fig. 1). Illuminating the specimen with a pattern of known spatial frequency has the property of replicating the spatial frequencies originating with the specimen at each of the illumination frequency peaks. In 'image space', this is analogous to Moire or beat patterns, the larger light/dark patterns that emerge when, for example, two window screens are superposed. In 'frequency space', the spectrum of spatial frequencies from the specimen is remapped to each of the frequency components of the illumination pattern (e.g. Fig. 1g), bringing some of the higher frequency components into the aperture [1,2]. Two general forms of structured illumination microscopy (SIM) have been developed for commercial implementation as super-resolution systems.

Wide-field structured illumination generally involves the projection of a sinusoidal excitation pattern onto the specimen with a period approaching the diffraction limit of the objective lens [1,3]. The sine wave at that spatial period in real space produces three peaks in frequency space, the zero order in the middle and two first-order components at opposite edges of the objective lens back aperture or 'frequency plane'. Since all of the spatial frequencies from the specimen are replicated and symmetrically mapped on to each of the three frequency components from the illuminating sine wave, new information is brought into the lens aperture from the two illumination frequency components closest to the aperture's edge (see Fig. 1a-p). Half of the symmetrically replicated and shifted spatial frequencies from the specimen are now broadcast back into the lens aperture from both first-order components. In this way, the lens captures twice the normal frequency information that can be applied to creating a 2-fold increase in spatial resolution. Shifting the sine wave pattern 3-5 times through 360° phase to completely illuminate the specimen and repeating this process at three different angles (0°, 120°, 240°) creates 9-15 images per focal plane. To extract the high-frequency information, the images are multiplied by matrix terms relating to the 3 or 5 phases of the translated illumination pattern [4]. A Fourier transform of each image is then shifted along the respective orientation axis and aligned using the three illumination peak positions from the structured illumination pattern forming what looks like a frequency space flower. A regularization filter is typically applied, using the frequency domain form of the PSF, the optical transfer function, to mitigate the highfrequency noise. A real image is then constructed using an inverse Fourier transform, scaled to an appropriate pixel size [1,2]. Conventional structured illumination in this form has been developed in 2D and 3D [4] using gratings or spatial light modulators to affect the structured illumination.

A second form of super-resolution SIM uses the inherently structured aspect of the scanned beam found in nearly all forms of confocal microscopy [5–7]. As the Airy disk formed by the diffraction-limited excitation beam is scanned over a fluorophore, the initial fluorescence is projected back to the detector producing a peak that is slightly off the optical axis (Fig. 1q-r). When the fluorophore becomes centered in the scanned excitation PSF, the emission PSF is focused back to the detector exactly on axis. When scanned further, the emission becomes off-axis again. Integration of the emission peaks with a point detector, such as a photomultiplier tube, produces a conventional confocal emission PSF. However, if the spatial information related to the off-axis peaks is collected as an image at each position separately on an array detector, such as a camera, the information can be shifted or reassigned to the 'true' position of the fluorophore, realizing a sqrt (2) improvement in resolution and a corresponding increase in brightness (Fig. 1s-u). Gaussian filtering the peaks prior to pixel reassignment (i.e. 'pinholing' [8]) provides a further increase in contrast and improved axial resolution. The collection of the off-axis information has been accomplished in a wide variety of hardware configurations. For a single scanned beam, a camera (i.e. ISM) or second galvonometric mirror and camera (i.e. rescan confocal) can sample the data into different pixels [5,9,10]. Alternatively, breaking a point detector into smaller spatial domains with non-Cartesian geometry (i.e. Zeiss Airyscan) provides a means for implementing super-resolution on an otherwise conventional confocal system. Parallelization of the excitation beam delivery, using a micromirror device [8], combined lenslet and pinhole arrays [11], spinning disk confocal [12-14] or engineered spinning disks (e.g. Olympus SpinSR10) with a high-speed camera has produced more rapid data acquisition with a similar sqrt(2) improvement in optical resolution.

Super-resolution imaging and plant cells

Super-resolution imaging in plant systems has been realized using a number of technologies applied to cells and isolated nuclei. Several contemporary reviews cover the extent of application and point to references for sample preparation [15–17]. While excellent demonstrations of subcellular structure and protein localization have been presented [18–20], super-resolution techniques, outside of applications to isolated nuclei, are only beginning to drive new areas of biological discovery in plant cells. Taking advantage of the increased resolving power of these techniques requires an increased level of attention to specimen preparation and knowledge of the underlying methods. The resulting data also require a new level of scrutiny by

authors and reviewers owing to the strong dependence on computational reconstructions and regularization techniques. The images synthesized from super-resolution approaches typically contain noise with a spatial structure that is different from the fluctuations observed at the single pixel level in conventional and confocal microscopy. Making explicit claims about the number and position of sub-diffraction elements from these data is an exciting and necessary evolution in our use of the light microscope [21], but subject to controls and careful attention to specimen preparation.

Super-resolution approaches applied to microbial and human tissue culture cells have taken excellent advantage of both immunohistochemistry and the introduction of alternative fluorescent labeling techniques in live cells [22]. The uniformly matched refractive index and protection from photobleaching afforded by modern mounting media dramatically improve all facets of the imaging process for fixed preparations. Chemical fixation and whole-mount labeling of plant cells is far more challenging owing to the pressurized nature of the cells, the relatively large liquid volume occupied by the vacuole, release of protease from the vacuole and the exclusion of antibodies and small molecules/dyes from cytoplasm by the intact cell wall. While excellent fixing and embedding protocols exist for some plant tissues, super-resolution techniques have been applied to whole-mount plant specimens in relatively few cases [16].

Plants are particularly challenging for super-resolution approaches because of the carbohydrate-dense wall surrounding the cell. Most flowering plants have cell walls with a refractive index that varies between 1.41 and 1.45. For living cells and fixed cells in an aqueous media, the curvature and varying thickness (50 nm–1 μ m) of the wall changes the optical path into, and out of, the cytoplasm. Refraction at the wall interface is strongly angle dependent and results in both a change in the direction of light propagation and angle-dependent polarization. Most plant cell walls additionally exhibit strong form birefringence owing to the cellulose microfibrils. When observed between crossed polars, the plant cell wall responds differently to polarized light applied in different orientations, dependent upon the degree and orientation of cellulose co-alignment.

Structured illumination methods rely extensively on the creation of a diffraction-limited excitation pattern to affect the higher order frequency information. The objective lenses commonly used for these approaches have a numerical aperture that extends light collection and illumination to a cone of nearly 170° for material with a refractive index close to glass. Light entering the plant cell and cell wall will undergo angle-dependent refraction unless the optical path is well matched for refractive index. Light

exiting the cell wall into the plant cytoplasm, where the refractive index is closer 1.34, will undergo further refractive changes ultimately leading to corruption of the structured illumination pattern. Using a mounting medium for fixed cells that matches the cell wall material (e.g. 60-80% glycerol) dramatically improves the illumination pattern [18] but may not control for polarization. Many two- and three-dimensional structured illumination approaches in wide-field systems use polarized excitation beams to form the interference pattern in the specimen and many laser scanning microscopes retain substantial linear polarization in the scanned beam. The birefringent cell wall interacts with the polarized light leading to corruption of the interference patterns in different orientations within the plant cell. Both the refractive index mismatch and the birefringence of the plant cell wall provide a significant challenge when attempting to create a uniform structured illumination pattern from multiple directions.

SIM at the plant epidermal cell cortex

The application of structured illumination to living plant cells has been most successful in the case of fluorescent proteins on the outer periclinal face of the epidermal cells [19]. The fluorescent emission from molecules at the cell cortex effectively lies within the optical field of the cell wall material. When the cell can be appressed to the cover glass, creating a relatively contiguous light path between glass and cell wall, the refractive index of the wall dominates the optical field. Compensation for the wall refractive index with an objective lens correction collar or a lower refractive index immersion oil can dramatically improve the fidelity of the illumination pattern and light collection. Use of compensating media for the plant, including various halocarbon oils or iodixanol [23,24], produces little gain in this regime for living cells because the cells are so close to the coverglass. Moreover, cell walls with strongly anisotropic cellulose distributions or substantial wax content still impair the formation of the structured illumination pattern.

Additional considerations apply to living plant cells related to the biology of the organism. The plant cytoplasm is typically streaming where cytoplasmic proteins are subjected to convective flow. Dependent upon movement rate, the time required to acquire a series of images for reconstructing an SIM image, often approaching 1 s, may be prohibitive relative to any gain in spatial resolution. Moreover, the requirement in wide-field SIM for equivalent images in at least three directions means that increasing the excitation energy to lessen exposure times will degrade the SIM image owing to progressive bleaching between orientations. Systems accumulating multiple

images from spinning disk or pinhole arrays share a similar fate when the images are recompiled from data that have bleached over the exposure time.

Structured illumination methods require using a defined pixel size relative to magnification for producing the extended Fourier field and returning the real space image. Correct spatial sampling typically requires intermediate magnification that spreads the emission from each diffraction-limited point over more pixels. While most point-scanning techniques, including iSIM, mSIM and Airyscan methods, effectively 'reassign' light that would be blocked or scattered to a smaller number of pixels, the increased noise incurred through collecting the light with a higher number of pixels still impacts base sensitivity. While signal is gained in the 'reassignment' of the light, a penalty is paid in noise coming from more independent sources. Hence, most SIM systems employ some form of regularization or deconvolution in post-processing to mitigate noise and improve high-frequency response. For plant cell imaging, the sampling issue compounds the problems for live cells. The number of photoelectrons accumulated per pixel needs to be large enough that the electronic noise from the pixel does not corrupt the reconstruction. Furthermore, the reliance on Weiner filters or iterative deconvolution methods to improve the signal to noise can be flawed for the plant case if imaging through the cell wall has produced an aberrant PSF, different than the expected PSF used in the noise filter. The appearance of mottle or spatially patterned background and the excessive ringing observed in SIM images are, thus, more difficult to suppress in the reconstructed image.

New information from existing probes

Linear structured illumination approaches, to date, provide 1.4–2-fold improvements to resolution in both lateral and axial dimensions using conventional fluorescent probes [25]. While still far from the molecular scale of individual proteins, observations on a ~100-nm scale provide a substantial amount of new information. Genetically encoded fusions of green fluorescent protein to various tubulin isoforms (e.g. GFP-TuB1) have provided insight into microtubule dynamics and function in living plant cells [26]. Epidermal light-grown hypocotyl cells, flattened against a cover glass to provide a direct optical path to the cortical microtubules attached to the plasma membrane, can be imaged with conventional (Fig. 2) and point-based (Fig. 3) SIM. Conventional wide-field structured illumination with a 488 nm excitation and 514 nm emission reveals polymers with an inhomogeneous fluorescence distribution having a 104 nm full width at half maximum (FWHM) intensity profile in the cross section using a 39.7 nm pixel size

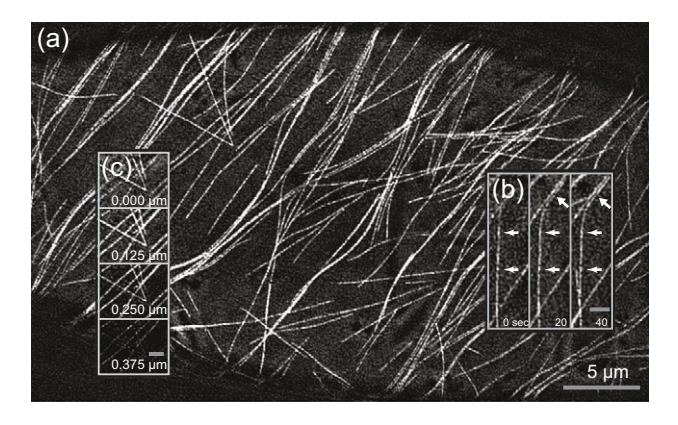


Fig. 2. SIM of cortical microtubules in living *Arabidopsis* hypocotyl cell. Single image plane from a light-grown 6-day-old seedling expressing a GFP-TuB1 transgene (a). Consecutive images taken after moving the specimen show the retention of irregular polymer labeling (b—long arrowheads) and formation of a bundle with resolved interbundle space (b—short arrowheads). Inset images of four consecutive image planes from one time point at 0.125 nm axial spacing (c) focusing into the cytoplasm. Note the prominence of the different microtubules in different axial planes indicating the 'stacking' arrangement of the polymers on the cell cortex. (DeltaVision OMX-SR with 63×1.42 NA objective lens reconstructing from 15 images per plane.) Bar in (b) and (c) = 2 μ m.

(Fig. 2). The irregular fluorescence distribution comes partly from the random incorporation of GFP-TuB1 subunits into the polymer (i.e. 'speckling') but also derives from the pattern noise in the imperfect reconstruction of the image, as evidenced by images taken after moving the specimen to different positions (Fig. 2b). The noise pattern is somewhat persistent where nearly the same pattern will appear in consecutive frames and through focus for a given sample, often leading to confusion about the underlying molecular distribution. Note that for this reason, the FWHM from Gaussian fitting to the intensity distribution serves as a convenient figure of merit but does not constitute the same information as a stated resolution limit. Two objects approaching each other at the sample plane will show an overlapping fluorescence intensity where the ability to define contrast between those objects in the image plane defines 'resolution'. Unlike the more typical fluctuation of intensity at the single pixel level (i.e. shot noise and detector noise) considered in most resolution tests [27], the noise pattern in the SIM reconstruction has a spatial scale that typically spans several pixels. The magnitude of that noise and its persistence between frames, therefore, merits careful consideration when estimating the mean contrast difference between fluorescent objects over a range of signal to noise values.

As established by electron microscopy [28,29], microtubules are 25 nm in cross section and interact at the cell cortex to form bundles that are offset by 25–30-nm spacer proteins [30]. The SIM image shows both the expected

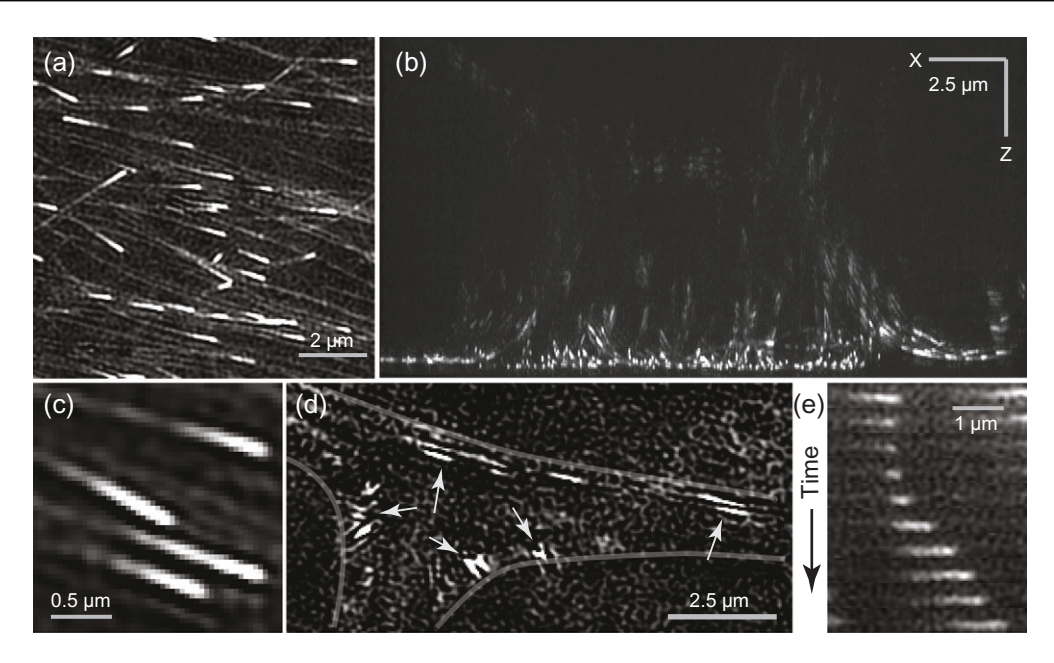


Fig. 3. Super-resolution imaging of microtubule End Binding-1 at the plant cell cortex using two structured illumination methods. Conventional SIM imaging of EB1-GFP in a living *Arabidopsis* hypocotyl cell in a 10-μm field of view shows distinctly resolved comets of different length (a). A side-on (XZ) projection of the same cell showing the rapid loss of signal for EB1-GFP foci along the anticlinal crosswall within 2 μm of the coverglass surface (b). Single-plane excerpt of EB1-GFP localization in a 2-μm field of view with individual 39.7 nm pixels (c) showing gradient of EB1-GFP tip localization and weaker labeling of the microtubule lattice. Single conventional SIM image at 4 μm depth showing the highlighted intersection of three cells (d). Arrowheads indicate the strongly asymmetric 'ringing' around EB1-GFP foci in the reconstruction relative to the orientation of the cell wall. ((a)—(d) using DeltaVision OMX-SR with 63×1.42 NA Oil immersion lens) Point-based SIM images of a single EB1-GFP-labeled microtubule tip over time (e) showing the loss of tip labeling as microtubule growth stalls and the reestablishment of the localization after recovery of polymer growth. (Olympus SD-OSR with 100×1.35 NA Silicone Oil immersion lens and Yokogawa W1 spinning disk).

sub-resolution (i.e. ~75 nm offset) microtubule bundles but additionally indicates contiguous resolved spaces between many bundling events indicating a potentially separate class of bundling phenomena (Fig. 1b). Examining the individual axial image planes from the 3D SIM data, constructed at 125-nm steps, the relative stacking position of microtubules that are laying across one another at the cortex can be determined by the gain and loss of signal in many cases (Fig. 2c). These data provide biological information that has been inaccessible through conventional microscopy and which gain substantially from having even a limited number of time-lapsed frames from the living cell to provide context.

A second genetically engineered probe, binding preferentially to the polymerizing ends of the microtubules (EB1-GFP), provides a different view of the cortical cytoskeleton (Fig. 3). Conventional wide-field SIM shows the distribution of the EB1-GFP fluorescence on the growing microtubule tips (Fig. 3a). The distribution of the EB1-GFP is partially slurred in the live cell image because the effective on/off rate of the protein is faster than the acquisition time for the 3D SIM image. A rotated projection of the 3D data set shows the loss of signal with axial depth owing to

refractive index mismatch for the EB1-GFP-labeled polymers following the anticlinal cell faces (Fig. 3b). Examination of an image plane more than a micrometer into the specimen shows the spatially oriented aberrations and asymmetric 'ringing' in the reconstruction where the structured illumination failed to evenly illuminate the EB1-GFP foci on different anticlinal side faces of the cell through the cell wall (Fig. 3c).

Structured illumination using a parallelized beam scanning approach can improve the speed of acquisition while sacrificing some of the improvement in spatial resolution [12]. A spinning disk was used to create super-resolution images of EB1-GFP at ~175 nm FWHM taken using a 300-ms acquisition (Fig. 3d), fast enough that the fluorescence is not appreciably slurred over the acquisition time. Images reconstructed at 1-s intervals show the cometshaped distribution of fluorescence changing over time as the growth of the microtubule polymer stalls and then recovers. The extended resolution of the imaging system provides more information about the molecular distribution along the polymer than conventional confocal microscopy. However, the improvement in spatial detail realized for objects just below the conventional diffraction limit

must be weighed against the introduction of pattern noise in the reconstruction. In this example, the confocal SIM image provides increased detail for understanding how the EB1-GFP localization changes as the polymer pauses and restarts growth. However, the noise pattern precludes use of the common assumptions regarding the distribution of fluorescence and obviates the use of conventional Gaussian-based approaches for fitting to the fluorescence distribution to determine sub-diffraction tip position [31].

Future development

Efforts to demonstrate super-resolution techniques in plant specimens have resulted in a number of successes. Yet, areas of plant cell biology, such as vesicle trafficking and actin organization, have vet to see widespread benefit from super-resolution approaches. Progress in the application of structured illumination techniques to plant systems for super-resolution will come from the combination of adaptive optics techniques [32,33] with computational deconvolution methods [34]. Deformable mirrors with dozens of piezo-actuators have the capacity to compensate for much of the wavefront aberration when placed in a conjugate plane to the back aperture of the objective lens [35]. Constructing the correct mirror deformation requires either a wavefront measurement or quantitative information about the PSF. Advances in hardware and wavefront sensor design have resulted in commercial implementations of adaptive optics for microscopy, where further development of software will make use more routine and applicable to compensating for the complex lensing effect of the plant cell wall.

The important goal of adaptive optics implementation is to restore the diffraction-limited performance of the imaging system. For structured illumination in plant systems, where the cell wall and its interface with the cytoplasm lead to substantial changes in the excitation wavefront, the compensatory action of the optic will improve the creation of the sinusoidal or spot pattern deeper into the specimen. Moreover, adaptive optics will improve the recovery of the emitted light and the formation of a corrected PSF. Restoration of a diffraction-limited PSF provides, in turn, an opportunity to apply PSF-based deconvolution methods that will genuinely improve the recovery of signal/noise at higher spatial frequencies, including mitigation of the noise patterns in the image background. Recalling that signal amplitude decreases with increasing spatial frequency in the microscope, newer approaches for computationally deconvolving the reconstructed image will improve the effective contrast so that the resolution can be realized in photon-limited fluorescence images [34].

Acknowledgements

The authors thank Drs Paul Goodwin, Peter Kner, Hari Shroff and John Sedat for input and discussions. DT and SLS thank the National Science Foundation for support including MCB:1615907 to SLS. DT was additionally supported through a James P. Holland Fellowship, a Carlos Miller Graduate Fellowship in Plant Biology, and a graduate fellowship from the Indiana University Graduate School in cooperation with the Templeton Foundation. Work was performed in the Indiana University Light Microscopy Imaging Center supported by NIH1S10OD024988-01.

References

- Gustafsson M G (2000) Surpassing the lateral resolution limit by a factor of two using structured illumination microscopy. *J. Microsc.* 198: 82–87.
- Heintzmann R, Jovin T M, and Cremer C (2002) Saturated patterned excitation microscopy—a concept for optical resolution improvement. J. Opt. Soc. Am. A. Opt. Image Sci. Vis. 19: 1599–1609.
- 3. Kner P, Chhun B B, Griffis E R, Winoto L, and Gustafsson M G (2009) Super-resolution video microscopy of live cells by structured illumination. *Nat. Methods* 6: 339–342.
- Gustafsson M G, Shao L, Carlton P M, Wang C J, Golubovskaya I N, Cande W Z, Agard D A, and Sedat J W (2008) Three-dimensional resolution doubling in wide-field fluorescence microscopy by structured illumination. *Biophys. J.* 94: 4957–4970.
- Muller C B, and Enderlein J (2010) Image scanning microscopy. Phys. Rev. Lett. 104: 198101.
- Sheppard C J, Mehta S B, and Heintzmann R (2013) Superresolution by image scanning microscopy using pixel reassignment. Opt. Lett. 38: 2889–2892.
- 7. Ward E N, and Pal R (2017) Image scanning microscopy: an overview. *J. Microsc.* 266: 221–228.
- 8. York A G, Parekh S H, Dalle Nogare D, Fischer R S, Temprine K, Mione M, Chitnis A B, Combs C A, and Shroff H (2012) Resolution doubling in live, multicellular organisms via multifocal structured illumination microscopy. *Nat. Methods* 9: 749–754.
- De Luca G M, Breedijk R M, Brandt R A, Zeelenberg C H, de Jong B E, Timmermans W, Azar L N, Hoebe R A, Stallinga S, and Manders E M (2013) Re-scan confocal microscopy: scanning twice for better resolution. *Biomed. Opt. Express* 4: 2644–2656.
- DE LUCA G M R, Desclos E, Breedijk R M P, Dolz-Edo L, Smits G J, Nahidiazar L, Bielefeld P, Picavet L, Fitzsimons C P, Hoebe R, and Manders EMM (2017) Configurations of the rescan confocal microscope (RCM) for biomedical applications. *J. Microsc.* 266: 166–177.
- York A G, Chandris P, Nogare D D, Head J, Wawrzusin P, Fischer R S, Chitnis A, and Shroff H (2013) Instant superresolution imaging in live cells and embryos via analog image processing. *Nat. Methods* 10: 1122–1126.
- 12. Azuma T, and Kei T (2015) Super-resolution spinning-disk confocal microscopy using optical photon reassignment. *Opt. Express* 23: 15003–15011.

- Roth S, and Heintzmann R (2016) Optical photon reassignment with increased axial resolution by structured illumination. Methods Appl. Fluoresc. 4: 045005.
- 14. Schulz O, Pieper C, Clever M, Pfaff J, Ruhlandt A, Kehlenbach R H, Wouters F S, Grosshans J, Bunt G, and Enderlein J (2013) Resolution doubling in fluorescence microscopy with confocal spinning-disk image scanning microscopy. *Proc. Natl. Acad. Sci. USA* 110: 21000–21005.
- Komis G, Novak D, Ovecka M, Samajova O, and Samaj J (2018) Advances in imaging plant cell dynamics. *Plant Physiol*. 176: 80–93.
- Schubert V (2017) Super-resolution microscopy—applications in plant cell research. Front. Plant Sci. 8: 531.
- Bell K, and Oparka K (2015) Preparative methods for imaging plasmodesmata at super-resolution. *Methods Mol. Biol.* 1217: 67–79.
- 18. Fitzgibbon J, Bell K, King E, and Oparka K (2010) Super-resolution imaging of plasmodesmata using three-dimensional structured illumination microscopy. *Plant Physiol.* 153: 1453–1463.
- Komis G, Mistrik M, Samajova O, Ovecka M, Bartek J, and Samaj J (2015) Superresolution live imaging of plant cells using structured illumination microscopy. *Nat. Protoc.* 10: 1248–1263.
- 20. Wanner G, Schroeder-Reiter E, Ma W, Houben A, and Schubert V (2015) The ultrastructure of mono- and holocentric plant centromeres: an immunological investigation by structured illumination microscopy and scanning electron microscopy. *Chromosoma* 124: 503–517.
- 21. Shaw S L, and Ehrhardt D W (2013) Smaller, faster, brighter: advances in optical imaging of living plant cells. *Annu. Rev. Plant Biol.* 64: 351–375.
- 22. Lavis L D, and Raines R T (2008) Bright ideas for chemical biology. ACS Chem. Biol. 3: 142–155.
- 23. Boothe T, Hilbert L, Heide M, Berninger L, Huttner W B, Zaburdaev V, Vastenhouw N L, Myers E W, Drechsel D N, and Rink J C (2017) A tunable refractive index matching medium for live imaging cells, tissues and model organisms. *eLife* 6: e27240.

- Littlejohn G R, Gouveia J D, Edner C, Smirnoff N, and Love J (2010) Perfluorodecalin enhances in vivo confocal microscopy resolution of *Arabidopsis thaliana* mesophyll. *New Phytol.* 186: 1018–1025.
- 25. Heintzmann R, and Huser T (2017) Super-resolution structured illumination microscopy. *Chem. Rev.* 117: 13890–13908.
- Ehrhardt D W, and Shaw S L (2006) Microtubule dynamics and organization in the plant cortical array. *Annu. Rev. Plant Biol.* 57: 859–875.
- 27. Stelzer E H K (1998) Contrast, resolution, pixelation, dynamic range and signal-to-noise ratio: fundamental limits to resolution in fluorescence light microscopy. *J. Microsc.* 189: 15–24.
- 28. Ledbetter M C, and Porter K R (1964) Morphology of microtubules of plant cells. *Science* 144: 872–874.
- 29. Zhang R, Alushin G M, Brown A, and Nogales E (2015) Mechanistic origin of microtubule dynamic instability and its modulation by EB proteins. *Cell* 162: 849–859.
- Smertenko A P, Chang H Y, Wagner V, Kaloriti D, Fenyk S, Sonobe S, Lloyd C, Hauser M T, and Hussey P J (2004) The Arabidopsis microtubule-associated protein AtMAP65-1: molecular analysis of its microtubule bundling activity. Plant Cell 16: 2035–2047.
- 31. Demchouk A O, Gardner M K, and Odde D J (2011) Microtubule tip tracking and tip structures at the nanometer scale using digital fluorescence microscopy. *Cell. Mol. Bioeng.* 4: 192–204.
- Debarre D, Botcherby E J, Booth M J, and Wilson T (2008)
 Adaptive optics for structured illumination microscopy. Opt. Express 16: 9290–9305.
- 33. Kam Z, Kner P, Agard D, and Sedat J W (2007) Modelling the application of adaptive optics to wide-field microscope live imaging. *J. Microsc.* 226: 33–42.
- 34. Arigovindan M, Fung J C, Elnatan D, Mennella V, Chan Y H, Pollard M, Branlund E, Sedat J W, and Agard D A (2013) High-resolution restoration of 3D structures from widefield images with extreme low signal-to-noise-ratio. *Proc. Natl. Acad. Sci. USA* 110: 17344–17349.
- 35. Booth M, Andrade D, Burke D, Patton B, and Zurauskas M (2015) Aberrations and adaptive optics in super-resolution microscopy. *Microscopy (Oxf)* 64: 251–261.